Publishing House
AKAPIT

COMPUTER METHODS IN MATERIALS SCIENCE

Informatyka w Technologii Materiałów

Vol. 11, 2011, No. 2

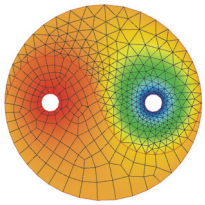

NUMERICAL SIMULATION OF FIELD DISTRIBUTION OF SERS ACTIVE SUBSTRATES FOR RHODAMINE 6G DETECTION

HUI-WEN CHENG, YIMING LI*

Department of Electrical Engineering, National Chiao Tung University, Hsinchu 300, Taiwan
**Corresponding author: ymli@faculty.nctu.edu.tw*

Abstract

In this work, we computationally study surface enhanced Raman spectroscopy (SERS) active substrates for the detection of Rhodamine 6G (R6G). To examine the electromagnetic enhancement, we first apply the finite-difference time domain (FDTD) algorithm to analyze the SERS active substrates by solving a set of Maxwell's equations (Ampere's Law and Faraday's Law) in differential form. The local field enhancements are simulated in the visible regime with the wavelength of 633 nm. Through the three-dimensional (3D) FDTD simulation, we find that the vertical variations have relatively larger field enhancement than that of horizontal variations. The roughened surface is then fabricated with a 12-hour hydrothermal treatment process and the measured strong Raman intensity, following the Beckmann-Kirchhoff theory, is significantly larger than that without hydrothermal treated sample.

Key words: SERS active substrate, Local field enhancement, Maxwell's equations, Nanoparticular, FDTD simulation, Hydrothermal synthesis, Raman shift, and Rhodamine 6G

1. INTRODUCTION

Surface enhanced Raman spectroscopy (SERS) has recently attracted a great deal of attention for rapid identification of chemical samples and molecules detection (Stiles et at., 2008; Jarvis, Goodacre, 2008). The simulation of field enhancement was done by several studies (Wang, D.-S., Kerker, M.). However, the analysis of simulated field enhancement of SERS active substrate is still lack. In this work, through the finite-difference time-domain (FDTD) method (Li & Cheng, 2009; Taflove & Hagness, 2000; Li & Cheng, 2008), we find that the degree of Raman enhancement strongly depends on the morphology of nanostructures. Then, we use hydrothermal treatment to roughen the surface of substrate (Yang et at., 2010). The measurement data shows that the surface enhanced Raman scattering signals from the surface of substrates with 12-hour treatment are larger than that of without treatment due to significantly rough and wide variation in structural surface.

This paper is arranged as follows. In Section 2, we state the computational model for the studied SERS active semiconductor substrate. In Section 3, we present the fabrication process of SERS active substrate and discuss the results from numerical simulation. Finally, we draw the conclusion and suggest future work.

2. THE NUMERICAL METHOD

Numerical simulation using a 3D FDTD method is conducted to investigate the local field enhancement of substrate. The Maxwell's curl equations in linear, isotropic, nondispersive, lossy materials are

$$\nabla \times E(x,t) = -\frac{\partial B(x,t)}{\partial t}, \qquad (1)$$

ISSN 1641-8581

$$\nabla \times H(x,t) = J(x,t) + \frac{\partial D(x,t)}{\partial t}, \qquad (2)$$

$$\nabla \cdot B(x,t) = 0, \qquad (3)$$

and

$$\nabla \cdot D(x,t) = \rho(x), \qquad (4)$$

where H and B are the magnetic field and induction, respectively, J and ρ are the electric current density vector and density of free charge. The electric and magnetic fields will be modified by materials. B describes how the material affects the magnetic field, and D describes how it affects electric field. For a globally defined curvilinear space, Maxwell's equations are easily implemented in their differential form, where Faraday's law is Eq. (1) and Ampere's law is Eq. (2).

In a non-conducting dielectric, current flow J = 0. Also, we have the following approximation:

$$B(x,t) = \mu H(x,t), \qquad (5)$$

where the magnetic permeability (μ) is a constant. In general, the electrical permittivity (ε) depends upon the frequency, but when the dependence is weak, it can be expressed as:

$$D(x,t) = \varepsilon E(x,t). \qquad (6)$$

The permittivity is a function of position. For example, in glass $\varepsilon \cong 1.2$. Assuming that Eqs. (5) and (6) hold, Maxwell's equations for a non-magnetic, non-conducting medium with no free charges or electrical currents is

$$\mu \frac{\partial H(x,t)}{\partial t} = -\nabla \times E(x,t), \qquad (7)$$

and

$$\varepsilon \frac{\partial E(x,t)}{\partial t} = -\nabla \times H(x,t). \qquad (8)$$

Now, we brief the finite difference (FD) approximation; the first derivative is approximated by

$$f'(x) \cong \frac{f(x+\frac{h}{2}) - f(x-\frac{h}{2})}{h}.$$

Using $d_x f(x) \cong f(x+\frac{h}{2}) - f(x-\frac{h}{2})$, the FD approximation to f' is $f'(x) \cong \frac{d_x}{h} f(x)$. Let $d = (d_x, d_y, d_z)$ and $\nabla f(x) \cong \frac{d}{h} f(x)$, where $\Delta x = \Delta y = \Delta z = h$. The second derivative is $f''(x) \cong \frac{d_x^2}{h^2} f(x)$ and $d_x^2 f(x) = f(x+h) + f(x-h) - 2f(x)$. Let $d^2 = d_x^2 + d_y^2 + d_z^2$, we have, $\nabla^2 f(x) \cong \frac{d^2}{h^2} f(x)$ and also replacing the derivatives of Maxwell's Eq. (7) by FD approximations we obtain $d_t H(x,t) = -\frac{1}{\mu}\frac{\Delta t}{h} d \times E(x,t)$. Here the electromagnetic field components are arranged on the grid in such a central FDs can be taken. Expanding $d_t H(x,t)$, and solving for $H(x, t+\frac{\Delta t}{2})$ gives $H(x,t+\frac{\Delta t}{2}) = H(x,t-\frac{\Delta t}{2}) - \frac{\Delta t}{\mu h} d \times E(x,t)$. Similarly, for Eq. (8) we have $d_t E(x,t+\frac{\Delta t}{2}) = -\frac{1}{\varepsilon(x)}\frac{\Delta t}{h} d \times H(x,t+\frac{\Delta t}{2})$ and $E(x,t+\Delta t) = E(x,t) - \frac{1}{\varepsilon(x)}\frac{\Delta t}{h} d \times H(x,t+\frac{\Delta t}{2})$ for Eq. (9).

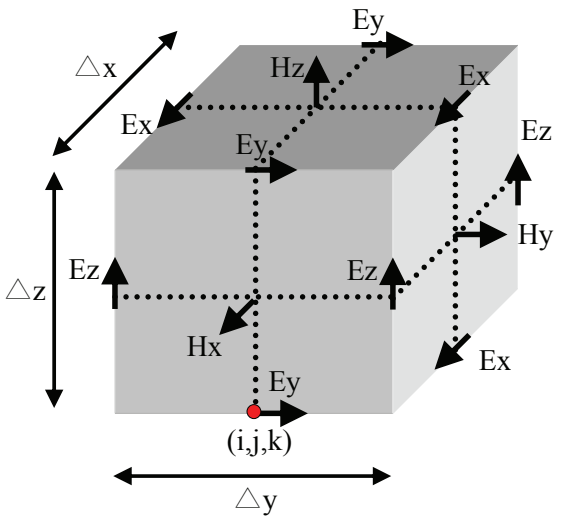

Fig. 1. *A Yee cell, where the H field is computed at points shifted one-half grid spacing from the E field grid points.*

The aforementioned equations are so-called the Yee algorithm (Yee, K., 1966), where the illustration is shown in figure 1. Each component of H and E is evaluated at a different, position. For example to compute $d_t H_z \sim d_x E_y - d_y E_x$, if H_z lies on (x, y, z) then E_y must be known at $(x \pm \frac{h}{2}, y, z)$, and

E_x at $(x, y \pm \frac{h}{2}, z)$, where the mathematical expressions are given by:

$$H^{n+1/2}_{x(i,j,k)} = H^{n-1/2}_{x(i,j,k)} + \frac{\Delta t}{\mu \Delta z}(E^{n}_{y(i,j,k)} - E^{n}_{y(i,j,k-1)}) - \frac{\Delta t}{\mu \Delta y}(E^{n}_{z(i,j,k)} - E^{n}_{z(i,j-1,k)}), \quad (9)$$

$$H^{n+1/2}_{y(i,j,k)} = H^{n-1/2}_{y(i,j,k)} + \frac{\Delta t}{\mu \Delta x}(E^{n}_{z(i,j,k)} - E^{n}_{z(i-1,j,k)}) - \frac{\Delta t}{\mu \Delta z}(E^{n}_{x(i,j,k)} - E^{n}_{x(i,j,k-1)}), \quad (10)$$

$$H^{n+1/2}_{z(i,j,k)} = H^{n-1/2}_{z(i,j,k)} + \frac{\Delta t}{\mu \Delta y}(E^{n}_{x(i,j,k)} - E^{n}_{x(i,j-1,k)}) - \frac{\Delta t}{\mu \Delta x}(E^{n}_{y(i,j,k)} - E^{n}_{y(i-1,j,k)}), \quad (11)$$

$$E^{n+1}_{x(i,j,k)} = E^{n}_{x(i,j,k)} + \frac{\Delta t}{\varepsilon \Delta y}(H^{n+1/2}_{z(i,j+1,k)} - H^{n+1/2}_{z(i,j,k)}) - \frac{\Delta t}{\varepsilon \Delta z}(H^{n+1/2}_{y(i,j,k+1)} - H^{n+1/2}_{y(i,j,k)}), \quad (12)$$

$$E^{n+1}_{y(i,j,k)} = E^{n}_{y(i,j,k)} + \frac{\Delta t}{\varepsilon \Delta z}(H^{n+1/2}_{x(i,j,k+1)} - H^{n+1/2}_{x(i,j,k)}) - \frac{\Delta t}{\varepsilon \Delta x}(H^{n+1/2}_{z(i+1,j,k)} - H^{n+1/2}_{z(i,j,k)}), \quad (13)$$

and

$$E^{n+1}_{z(i,j,k)} = E^{n}_{z(i,j,k)} + \frac{\Delta t}{\varepsilon \Delta x}(H^{n+1/2}_{y(i+1,j,k)} - H^{n+1/2}_{y(i,j,k)}) - \frac{\Delta t}{\varepsilon \Delta y}(H^{n+1/2}_{x(i,j+1,k)} - H^{n+1/2}_{x(i,j,k)}). \quad (14)$$

Notably, we employ the perfectly matched layer as the simulation domain boundaries in which both electric and magnetic conductivities are introduced in such a way that wave impedance remains constant, absorbing the energy without inducing reflections.

The field enhancement of SERS active substrate with gold-coated nanopartcle is obtained by solving the Maxwell's equations above. We use the derived FDTD method to solve Maxwell's equations by first discretizing all equations via central differences in time and space. Then, based upon the 3D Yee's mesh and components of the electric and magnetic fields at points, the discretized spacing in the x, y, and z directions adopted in our simulation are $|x|$ = 0.01 μm, $|y|$ = 0.01 μm and $|z|$ = 0.01 μm, where the time step Δt is 0.0004 and the time duration T is 3 in units of femtoseconds. The discretized equations are iteratively solved in a leapfrog manner, alternating between computing the E and H fields at subsequent $\Delta t/2$ intervals, as shown in figure 2.

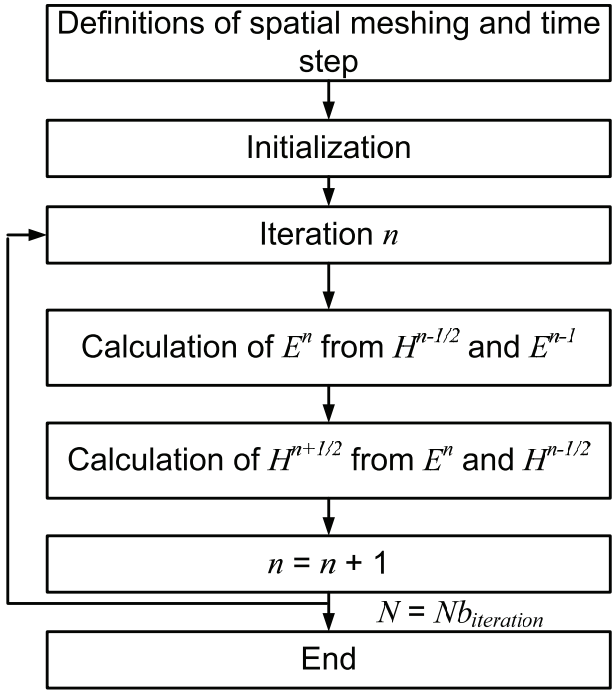

Fig. 2. Illustration of the FDTD simulation procedure for the local filed problem of SERS active substrate for R6G under the wavelength of 633 nm.

3. RESULTS AND DISCUSSION

3.1. Numerical simulation

Through using FDTD method, the evaluation of electric field on the substrates is carried out by directing light with a wavelength of 633 nm, where the matrix of simulated nanoparticles structure is 3 x 5 due to periodical property of the fabricated structure, as shown in figure 3(a). The mesh plots of the simulated structure are shown in figures 3(b) and 3(c), where the computational time of a single case is about 14 minutes. The effect of vertical variation of surface on the electric field (E_x) enhancement can also be observed from figure 4. The simulation result shows that the gold-coated nanoparticular structure with hydrothermal treatment (upper plot) has larger electrical field than that without hydrothermal treatment (lower plot).

(a)

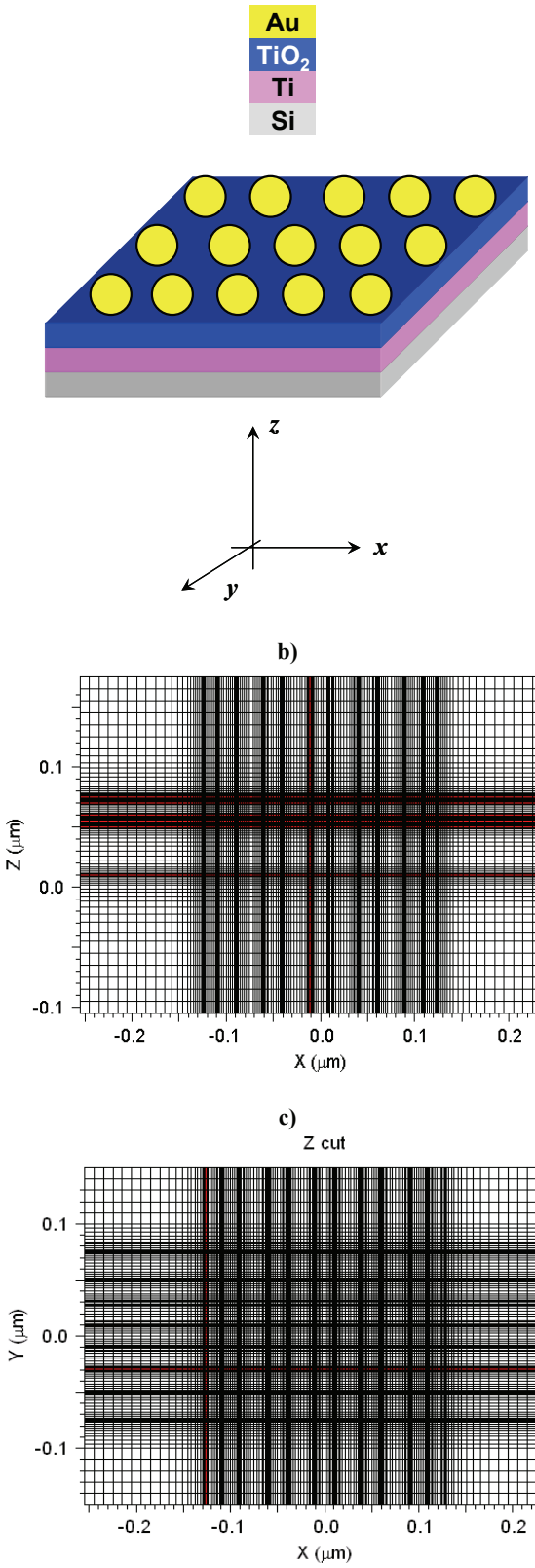

Fig. 3. *(a) The matrix size of particles is 3 × 5 accordingly to an approximately periodical assumption of the simulated structure; the simulation domain in the x-y plane is 0.4 um × 0.2 um. (b) and (c) are the plots of mesh of the simulated structure in the x-z and x-y planes, respectively.*

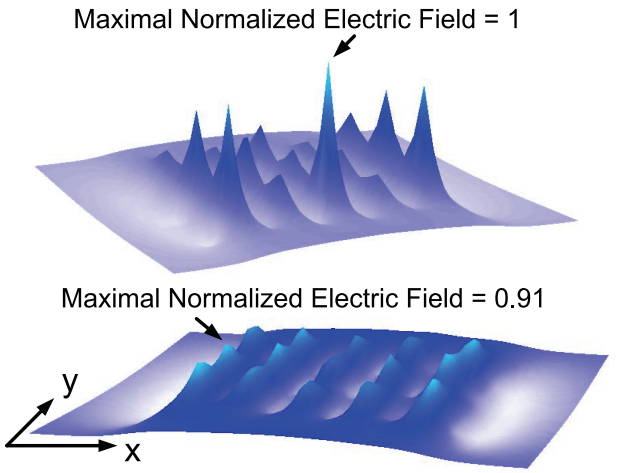

Fig. 4. *The upper and lower plots show the FDTD simulated electric fields of the examined substrate with and without roughened surfaces, respectively.*

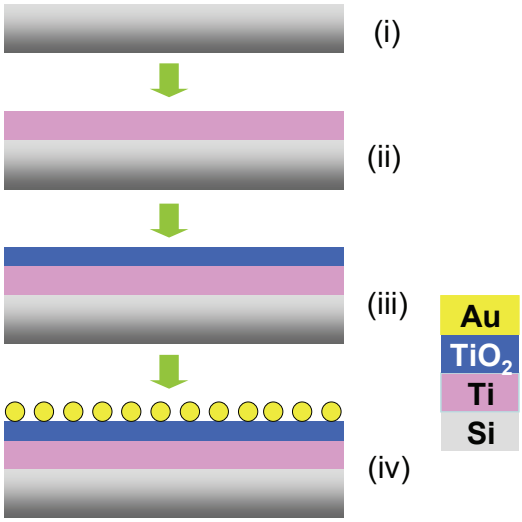

Fig. 5. *Schematic representation for the fabrication of SERS-active substrate. First, silicon wafers were cleaned by BOE and standard RCA cleaning procedures. Then, Ti films were deposited on the pre-cleaned silicon wafers using reactive DC magnetron sputtering system. The as-deposited samples were cleaved and treated under hydrothermal conditions for various durations. Subsequently, Au was thermal evaporated onto the hydrothermally roughened substrates for sensing.*

3.2. Sample fabrication and measurement

Based upon our numerical simulation results, the roughened surface of substrate is predicted to have larger field enhancement. Therefore, we develop a new fabrication method, so-called the hydrothermal treatment, to achieve it. The flow of fabricated substrate with gold-coated nanoparticle treated by hydrothermal method is shown in figure 5. First, buffered oxide etchant (BOE) and standard RCA cleaning are carried out to prepare clean silicon substrates (Boron-doped p<100>). Then, 100-nm-thick titanium films are deposited on the pre-cleaned silicon wafers using reactive DC magnetron sputtering

system. The as-deposited sample is cleaved into 0.5 cm × 1 cm squares and rinsed with ethanol, and de-ionized water.

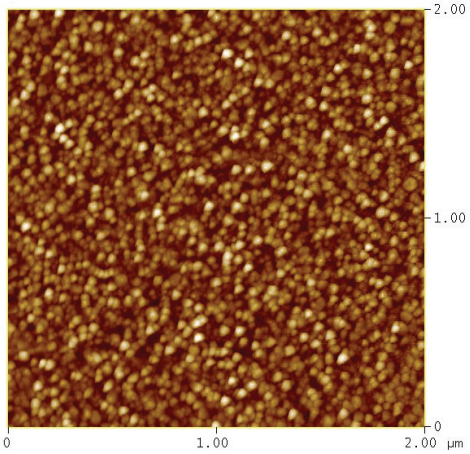

Fig. 6. *The AFM image of titanium thin films treated under hydrothermal condition for 12 hours treatment duration.*

Subsequently, the sample is put into a 23 mL Teflon-lined stainless steel autoclave filled with 20 mL distilled water, which is sealed, and heated at 200°C for 2, 4, 6, 8, 10, and 12 hours, respectively. Then the treated sample is cooled to room temperature naturally, washed with distilled water for several times, and dried with a stream of cylinder air. For example, figure 6 shows the AFM images represent titanium thin films treated under hydrothermal conditions for 12 hours treatment duration.

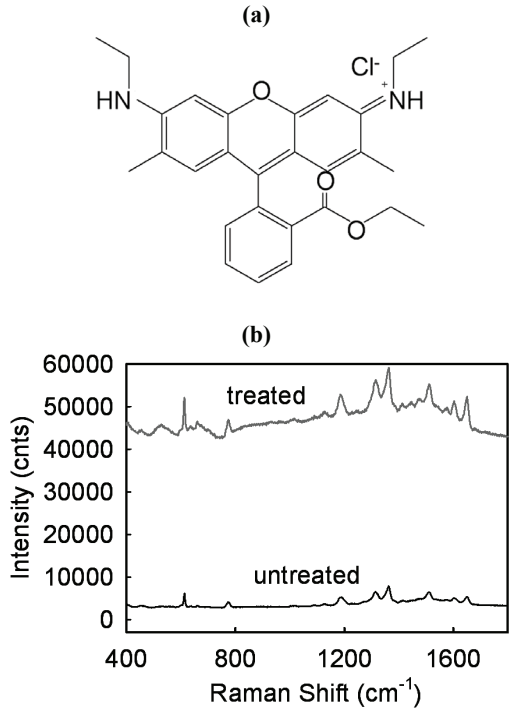

Fig. 7. *(a) Chemical structure of Rhodamine 6G (R6G). The molecule is widely used for SERS measurements. (b) The Raman spectra for R6G (10^{-4} M) immobilized on hydrothermally untreated (red) and treated (green) substrates.*

For chemical sensing, the hydrothermally roughened substrates are treated with aqueous solutions of 10^{-4}M R6G where the structure is shown in figure 7(a). Figure 7(b) shows the characteristic Raman vibrational modes of R6G immobilized on the substrate with or without hydrothermal treatment. The results show that the substrate with hydrothermal treatment shows larger intensity than that without hydrothermal treatment which can be explained by Beckmann-Kirchhoff theory (Beckmann, & Spizzichino, 1963) due to the roughness on the surface.

4. CONCLUSIONS

In this study, the field enhancement of SERS active substrate with gold-coated nanoparticle has been calculated by solving a set of 3D Maxwell's equations. The computational estimation of local field enhancement using FDTD method has confirmed the detected large intensity of Raman shift which indicates a clear view of such enhancement is resulted from vertical variations of the grown film. With prediction from the simulation results, the hydrothermal synthesis technique is developed to achieve roughened surface of SERS-active substrate for R6G sensing. We are currently studying the geometry effect on the local field enhancement for biomedical and chemical sensing applications.

ACKNOWLEDGEMENT

This work was supported in part by National Science Council (NSC), Taiwan under Contracts No. NSC-97-2221-E-009-154- MY2 and No. NSC-99-2221-E-009-175.

REFERENCE

Beckmann, P., Spizzichino, A., 1963, *The scattering of Electromagnetic Waves from Rough Surfaces,* Pergamon Press, Oxford.

Jarvis, R.M., Goodacre, R., 2008, Characterization and identification of bacteria using SERS, *Chem. Soc. Rev.*, 37, 931-936.

Li, Y., Cheng, H.-W., 2008, Numerical simulation of field emission efficiency of anodic aluminum oxide carbon nanotube field emitter in the triode structure, *Comp. Phys. Commun.*, 179, 107-111.

Li, Y., Cheng, H.-W., 2009, Optimal Configuration of Hydrogen-Embrittlement-Fabricated Nanogaps for Surface-Conduction Electron-Emitter Display, *IEEE Trans. Nanotech.*, 8, 671-677.

Stiles, P.L., Dieringer, J.A., Shah, N.C., Van Duyne, R.P., 2008, Surface-enhanced Raman spectroscopy, *Annual. Rev. Analyt. Chem.*, 1, 601-626.

Taflove, A., Hagness, S.C., 2000, *Computational Electrodynamics: The Finite-Difference Time-Domain Method*, 2nd ed., Artech House, Boston, MA.

Wang, D.-S., Kerker, M., 1981, Enhanced Raman scattering by molecules adsorbed at the surface of colloidal spheroids, *Phys. Rev*., B 24, 1777-1790.

Yang, J.-Y., Cheng, H.-W., Chen, Y., Li, Y., Lin, C.-H., Lu, K.-L., 2010, Novel hydrothermal roughened nanostructured substrates for biological and chemical detections, *J. Nanosci. Nanotech.*, in press.

Yee, K., 1966, Numerical solutions of initial boundary value problems involving Maxwell's equations in isotropic media, *IEEE Transactions on Antennas and Propagation*, AP-14, 302-307.

NUMERYCZNA SYMULACJA ROZKŁADU AKTYWNYCH SKŁADNIKÓW DO WYKRYWANIA RODAMINU 6G METODĄ SPEKTROSKOPII RAMANA

Streszczenie

W pracy przeprowadzono numeryczną analizę rozkładu aktywnych substratów stosowanych w spektroskopii Ramana (ang. surface enhanced Raman spectroscopy - SERS) do wykrywania rodaminu 6G. Aby wyznaczyć wzmocnieni elektromagnetyczne w pierwszej kolejności zastosowano metodę różnic skończonych w czasie (ang. finite-difference time domain - FDTD). Metodą tą analizowano rozkład aktywnego substratu w metodzie SERS poprzez rozwiązanie układu równań Maxwella (prawo Ampera i prawo Faradaya) zapisanego w formie różnicowej. Lokalne wzmocnienie pola symulowano w paśmie widzialnym o długości fali 633 nm. 3D symulacje metodą FTDT pokazały, że zmiany pionowe dają większe wzmocnienie pola niż zmiany poziome. Szorstka powierzchnia jest następnie wytwarzana poprzez 12-godzinną obróbkę hydrotermiczną. Obserwowany znaczny wzrost natężenia Ramana, zgodnie z teorią Beckmann-Kirchhoffa, jest znacznie większy niż bez tej obróbki.

Received: October 11, 2010
Received in a revised form: December 20, 2010
Accepted: December 23, 2010